

Technical Note

Summary The moisture distribution within a space and the degree to which moisture movement can be modelled using tracer gas techniques and computational fluid dynamics (CFD) models are examined. The validity of these methods to study moisture migration is examined experimentally in an environmental two-zone test chamber. It is found that molecular diffusion plays a very small role in airborne moisture movement. Thus airborne moisture migration is primarily affected by air movement. The major influences are the shape of the buoyant plume and the position of air supply and extract in relation to the moisture source location.

Moisture movement: A study using tracer gas techniques and CFD modelling

M Kolokotroni DipArch MSc PhD, N Saiz BSc and J Littler MA PhD CEng MCIBSE MCI(OB)
 Research in Building Group, Polytechnic of Central London, 35 Marylebone Road, London NW1 5LS, UK

Received 14 October 1991, in final form 6 December 1991

1 Introduction

Condensation is a major problem in a large number of dwellings in the UK⁽¹⁾ and other cold climates. The reduction of ventilation levels for energy conservation coupled with low internal temperatures in some parts of a dwelling have increased condensation problems in many cases. The importance of ventilation in reducing condensation risks and the importance of the local removal of moisture at source have been long recognised, and recently implemented in the current Building Regulations⁽²⁾.

Most of the available prediction models deal with the average relative humidity of a space⁽³⁻⁵⁾ and do not take into account the moisture distribution within a space, which is an important consideration especially during periods of water vapour production. In this article, the degree by which water vapour concentration differs within a space in transient mode as well as the effects of air movement on the distribution are investigated.

The computational fluid dynamics (CFD) model FLO-

VENT⁽⁶⁾ and an environmental two-zone test chamber are used as research tools. FLOVENT was chosen because it is a CFD code developed specifically for applications in buildings, and can be used in a variety of computer platforms in a form accessible to designers and engineers with a convenient input and output. Water vapour was introduced (as a contaminant and heat source) into the space and its distribution studied at a large number of grid points in three dimensions. The CFD model does not consider condensation, evaporation or adsorption/desorption, and so the simulation conditions were chosen so that the vapour saturation point was not reached, in order to avoid unrealistic concentrations.

The CFD model has been reproduced by experiment in the environmental two-zone test chamber available at PCL, by lining the walls of the inner cell with aluminium foil to prevent any hygroscopic adsorption or condensation on the walls. The chamber is divided by a partition into two similar cells. The partition has a lower and an upper opening and there is a calibrated flushing fan between the two cells (Figure 1). Water vapour is produced by a calibrated elec-

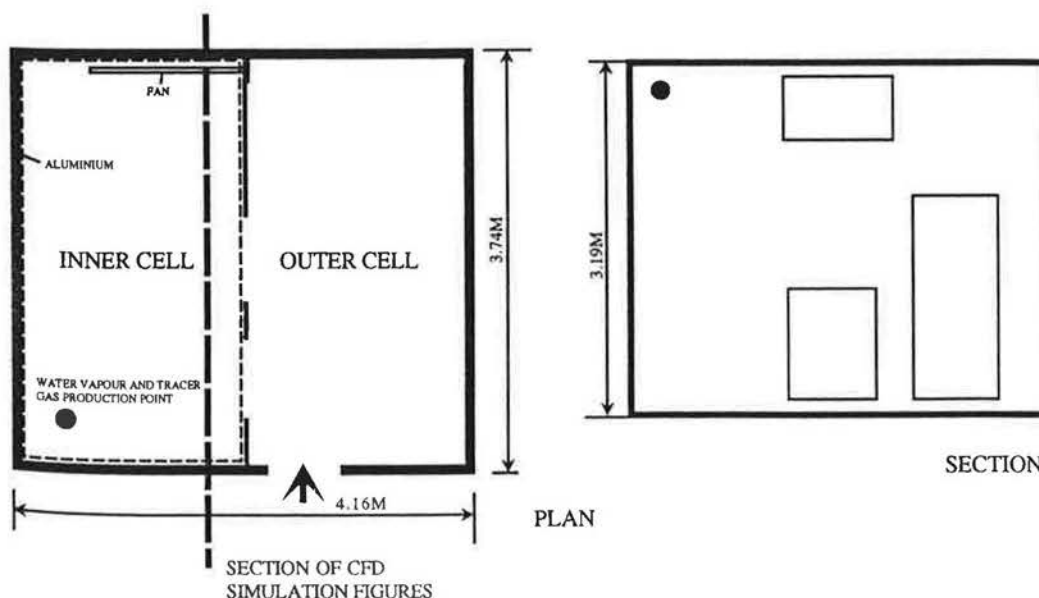


Figure 1 Two-zone environmental chamber

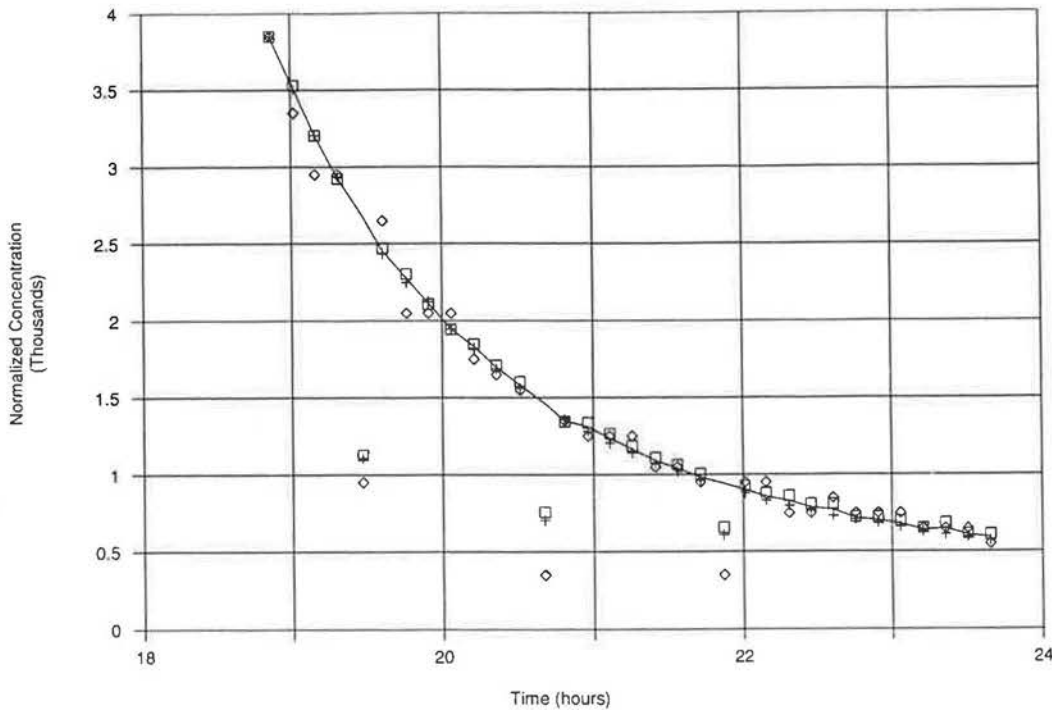


Figure 2 Simultaneous measurements of the decay curves of water vapour (\diamond), freon (+) and SF_6 (\square) in the aluminium-lined inner cell, showing that the three gases behave similarly when there is no hygroscopic adsorption. Groups of points well below the curve are concentrations in the outer cell.

trical immersion heater. In addition, tracer gases are used in some of the experiments using both concentration decay and constant rate of injection methods to measure ventilation and to compare with the water distributions and the simulation results.

2 Tracer gases and water vapour

The water and tracer concentrations were measured with an infra-red photoacoustic detector (Brüel & Kjaer type 1302) sampling air drawn through tubes via a 16-way automated valve, giving concentrations accurate to three significant figures. Temperatures were measured by thermocouples and a data logger, and are accurate to 0.1°C .

A graph of simultaneous measurements of two tracer gases (sulphur hexafluoride and freon R113, relative molecular masses 146 and 187 respectively) and water vapour is presented in Figure 2. The tracer gas concentrations have been normalised to the water vapour concentration above the background level by a constant multiplier. The experiment was carried out in the aluminium-lined inner cell so that water adsorption was eliminated. Also, the water vapour concentration was kept low to avoid condensation. All three gases were released into the cell and were mixed continually by two fans. Meanwhile a slight overpressure and an air change rate of about 0.85 h^{-1} were maintained in the cell by the flushing fan. The lower opening was open by 0.44 m^2 , through which the gases flowed and diffused. This arrangement provides well mixed air/tracers over the entire open area, allowing diffusion to occur in three dimensions.

It was observed that the water vapour and the two tracer gases decayed at very similar rates. The three groups of points in Figure 2 not following the decay curve are concentrations in the outer cell, which had no aluminium lining. The tracer gases are still in good agreement; however, the water vapour concentrations are reduced by adsorption in the outer cell. The three gases have very different diffusivities (water diffuses about four times as fast as the two tracers), and so this graph is evidence that 'molecular

diffusion' plays a very small role in water transfer, under these conditions, which are not unrealistic for kitchens and bathrooms.

3 Time-dependent water vapour concentration

The time-dependent vapour distribution within a space was studied by examining the rise of humidity during a moisture production period (typically of 30 min) and the decay of humidity afterwards (typically for a further 90 min). This has been examined experimentally in the environmental test chamber and using the CFD model.

The main bulk of the experimental work was carried out on the periods of rising and falling concentrations in the inner room of the environmental chamber. An example of the experimental results measured in the inner cell before it was lined with aluminium is shown in Figure 3. It can be seen that during the first 2.5 hours, the concentration rose close to steady state. Most of the room is at a very high concentration, except for the lower part where the incoming air becomes stratified. When the vapour production ceases, the air in the room mixes and there is a more gentle concentration gradient in the room. The graph also shows how the concentration close to the ceiling is slightly lowered due to hygroscopic adsorption.

The experimental chamber was also simulated by the CFD model. Water vapour was modelled as a contaminant (introduced with a heat source) with a density equal to the air. Thus, the current model assumes that the contaminant is carried purely by airflows.

The vapour distribution was examined at two distinct times: (a) at the end of a 30 min period, during which vapour was produced at a rate of 0.083 g s^{-1} (150 g over 30 min) and (b) at 120 min, i.e. 90 min after moisture production was stopped. The lower opening of the partition wall was open to give an opening of 0.5 m^2 . Initial conditions were 0.006 kg/kg dry air vapour content and 20°C temperature, i.e. 40% RH. A vertical section parallel to the internal wall of the room is presented for the two times in Figures 4 and 5,

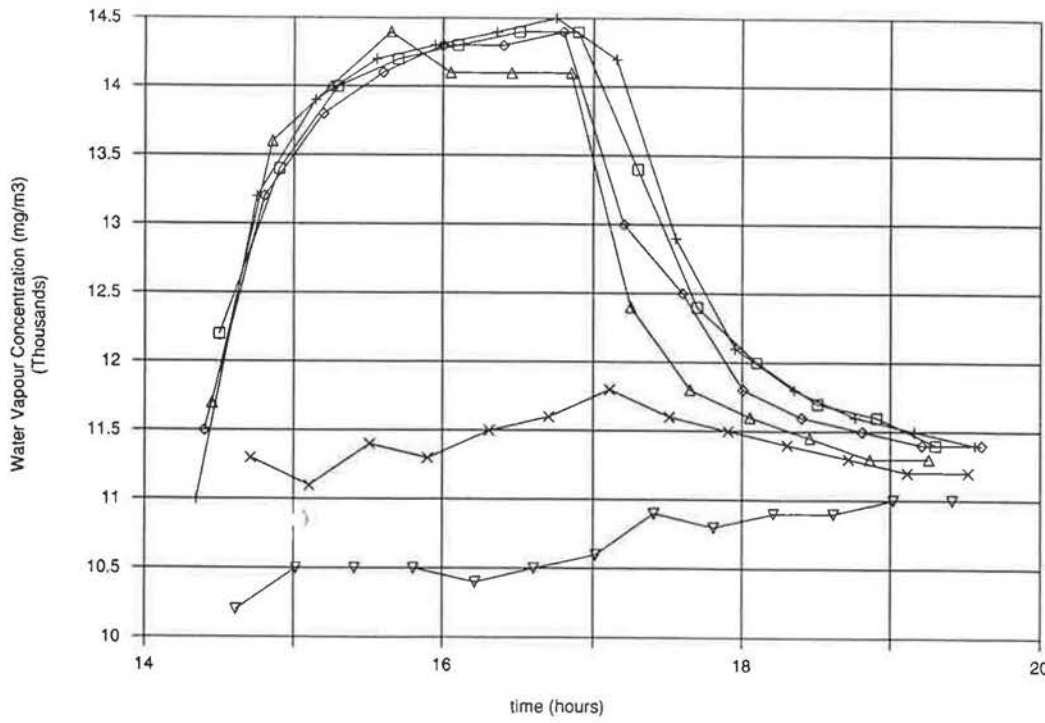


Figure 3 Measured water vapour concentrations at the five heights 0.9 m (x), 1.5 m (Δ), 2.35 m (◇), 2.9 m (+), 3.2 m (□) in the middle of the inner cell of the environmental chamber before it was lined with aluminium foil. ▽ denotes the outer cell concentration.

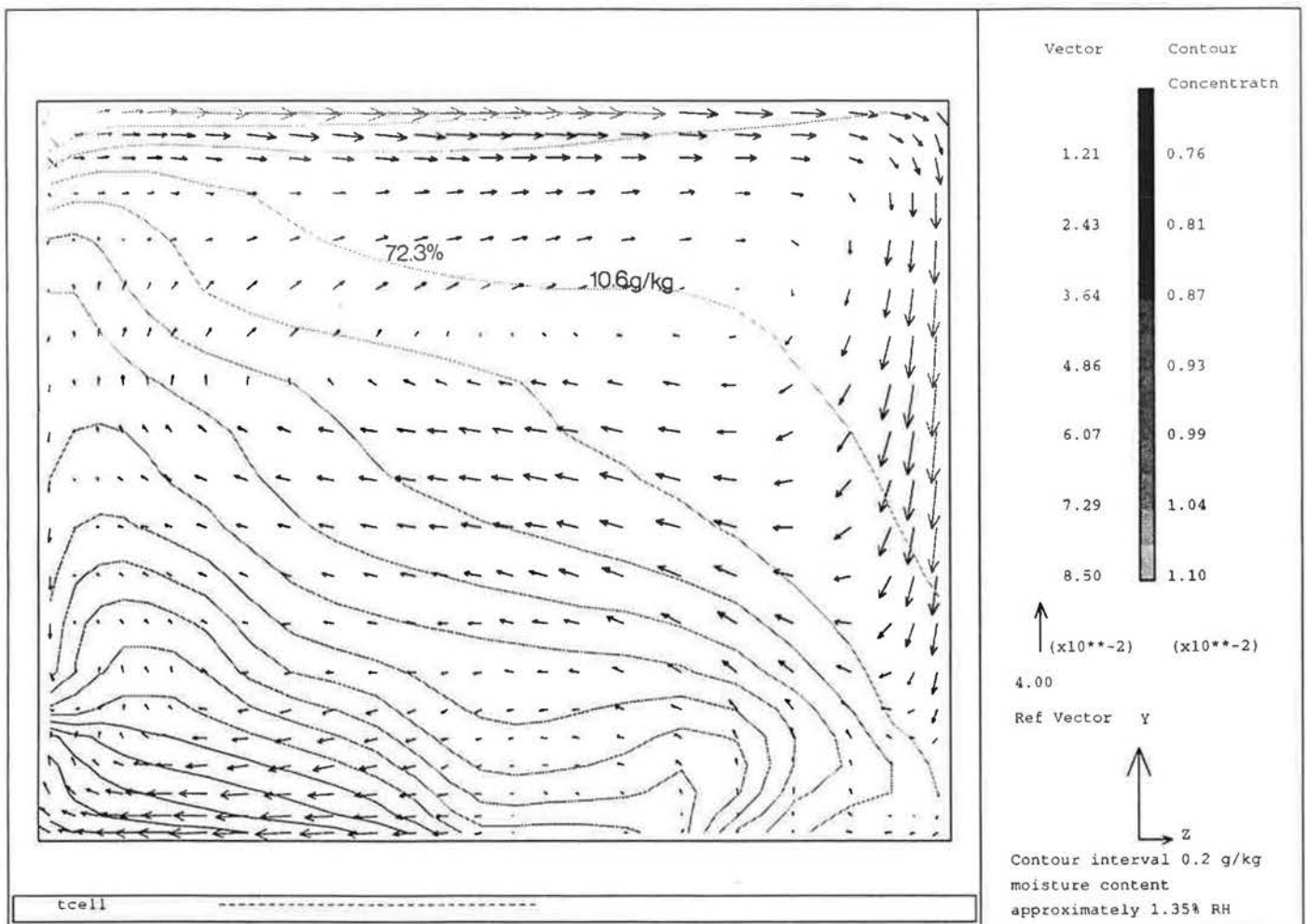


Figure 4 CFD modelling: Moisture content-RH contours and air flow vectors at the end of water vapour production

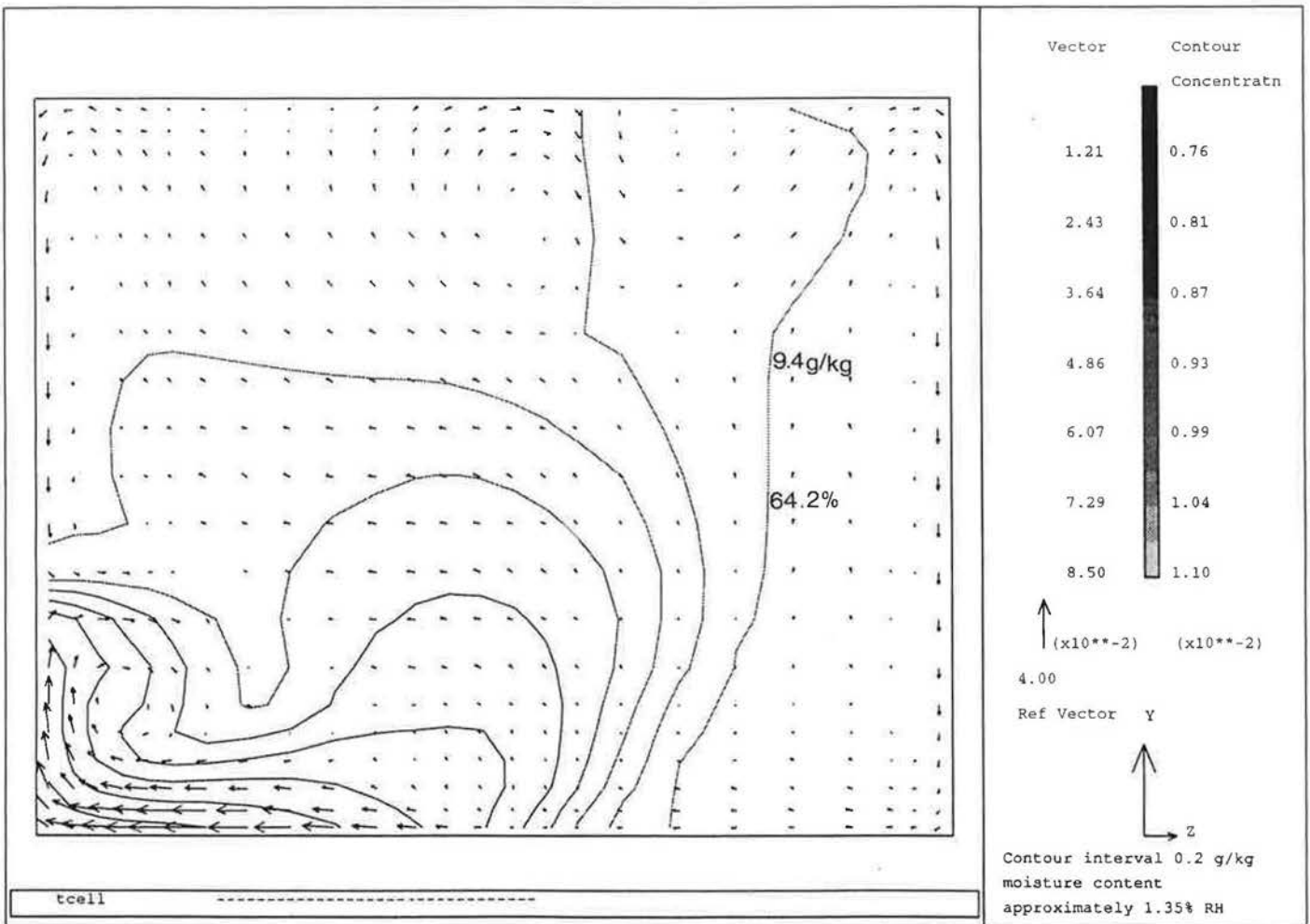


Figure 5 CFD modelling: Moisture content-RH contours and air flow vectors 90 min after the end of vapour production

where the air flow vectors and vapour contours are shown. Although the CFD model calculates moisture content only, the corresponding RHs are also marked on the figures, as RH is the parameter usually measured and the important factor for mould growth. The temperature variation in this particular simulation run is negligible (differences of less than 0.2°C, apart from the source).

It was found that there exist vertical and horizontal vapour distributions which are greatest during the period of vapour production (Figure 4) and also marked during the decay period (Figure 5). Preliminary results suggest that there are differences of 3 g/kg air (20% RH) during vapour production and 2.2 g/kg air (15% RH) at the end of a long decay period. It is important to note that the variations appear in both horizontal and vertical planes and are mainly due to the effects of air flows within the space, signifying the importance of an appropriate extract position and sufficient extractor fan capacity for the effective removal of excess water vapour.

4 Conclusions

The main experimental and simulation findings to date are as follows.

The position of the opening has a marked effect on vapour distribution and concentration, although a vertical dis-

tribution with lower values near the floor and higher values near the ceiling is always observed. The difference between floor and ceiling vapour concentrations is greater than 20% in most cases. In addition, greater differences in horizontal concentration distribution were observed (in excess of 40% in some cases), with the highest values not always near the moisture source. The positions of air inlet and extract play an important role in the build-up and decay of vapour in particular locations within a space.

Vapour distribution is primarily affected by air movement. The major influences are the shape of the buoyant plume and the positions of supply and extract of air.

During periods of vapour production, there is a well mixed upper layer of very humid air whose depth generally increases with vapour production and decreases with ventilation. The lower boundary of this layer forms near the ceiling and falls until it is about level with the point of extraction.

The hygroscopic depletion layer (due to airborne moisture being adsorbed onto the surfaces) is very near the surface, i.e. there is a local minimum humidity at around 1–2 cm from the wall and 10 cm from the wall there is no noticeable effect. This layer is dominated by diffusion, since the air is stagnant near the surfaces, and so the humidity is coupled more closely to the surfaces than the room bulk air. When the walls are 'wetter' than the air the effect is reversed and this layer is more damp than the bulk air in the room.

These findings underline the importance of moisture extraction during production time, preferably at areas of highest concentration, usually near the moisture source and the ceiling. In this way a greater amount of moisture can be extracted for a given ventilation rate. This is compatible with the normal practice of locating extractor fans at high level, but less attention is paid by installers to the proximity to the moisture source. Therefore the horizontal distribution at different time steps for various air extraction and moisture production locations will be investigated in detail using CFD modelling, the environmental chamber and occupied dwellings.

The work reported in this article forms part of a broader research project dealing with the study of airborne moisture movement and its effects on condensation risks in dwellings. More work is being carried out on transfer mechanisms, particularly on the importance of 'turbulent diffusion'. Further work will produce a moisture balance algorithm to be incorporated in a mould prediction computer model⁽⁵⁾ which calculates a time-averaged humidity in the whole house. Our program will split the dwelling into a number of zones, each with its own humidity and mould risk algorithm. It will also be able to predict the moisture distribution within a zone in relation to the location of moisture source and openings, from a calculated average concentration predicted using simple steady-state equations^(7,8) or a measured value in the middle of the zone.

Adsorption data from other sources such as BRE and IEA

will be considered in the algorithm. Finally, advice on extract fan capacity will be offered on the basis of our case studies.

Acknowledgements

The authors wish to thank Dr T Oreszczyn of the Bartlett UCL and Chris Sanders of BRE Scotlab for useful advice. Thanks are also due to BSRIA and Flomerics for help with FLOVENT. This work is supported by SERC.

References

- 1 Sanders CH *Dampness data in the 1986 English House Condition Survey* International Energy Agency—Annex XIV: Report UK-T7-35/1989 (1989)
- 2 *The Building Regulations 1985 Part F1 Means of Ventilation* (London: HMSO) (July 1989)
- 3 Yuguo L Moisture Content of Kitchen Air in a Multi-Room Residence *Climate and Buildings* 1(1) 36–44 (1990)
- 4 Fairey P and Kerestecioglu A Dynamic Modelling of Combined Thermal and Moisture Transport in Buildings: Effect on Cooling Loads and Space Conditions *ASHRAE Trans.* 91(2) (1985)
- 5 Boyd D, Cooper P and Oreszczyn T Condensation Risk Prediction: the Addition of a Condensation Model to BREDEM *Building Serv. Eng. Res. Technol.* 9(3) 117–125 (1988)
- 6 *FLOVENT Reference Manual* (London: Flomerics Limited) (1991)
- 7 *Condensation and Energy* IEA Annex XIV (Leuven-Heverlee, Belgium: International Energy Agency) (1991)
- 8 *Control of Condensation in Buildings* British Standards Institution Code of Practice BS5250 (London: British Standards Institution) (1989)